Supersymmetric laser arrays

R. El-Ganainy*
Department of Physics, Michigan Technological University, Houghton, Michigan 49931, USA

Li Ge
Department of Engineering Science and Physics, College of Staten Island, CUNY, Staten Island, New York 10314, USA and The Graduate Center, CUNY, New York, New York 10016, USA

M. Khajavikhan and D. N. Christodoulides
College of Optics & Photonics–CREOL, University of Central Florida, Orlando, Florida 32816, USA
(Received 8 December 2014; published 11 September 2015)

We introduce the concept of supersymmetric laser arrays that consist of a main optical lattice and its superpartner structure, and we investigate the onset of their lasing oscillations. Due to the coupling of the two constituent lattices, their degenerate optical modes form doublets, while the extra mode associated with unbroken supersymmetry forms a singlet state. Singlet lasing can be achieved for a wide range of design parameters, either by introducing stronger loss in the partner lattice or by pumping only the main array. Our findings suggest the possibility of building single-mode, high-power laser arrays and are also important for understanding light transport dynamics in multimode parity-time symmetric photonic structures.

DOI: 10.1103/PhysRevA.92.033818 PACS number(s): 42.55.Sa, 42.55.Ah, 42.60.Da

I. INTRODUCTION

Supersymmetry (SUSY) was proposed as a unifying theme that treats bosonic and fermionic particles on equal footing [1]. Later, this notion was applied to quantum mechanics, scattering processes, and nonlinear dynamics [2]. By noting that SUSY transformations are not pertinent to quantum field theory, similar concepts were also applied to quantum cascaded lasers [3]. Recently, it was recognized that SUSY can be employed to achieve unprecedented control over light transport in optical guiding geometries [4] where mode conversion in passive SUSY optical waveguide arrays has been experimentally demonstrated [5].

Another field that has received much attention recently is pump-induced mode selection in integrated laser systems [6–11]. In these works, it was shown that laser emission of certain modes can be enhanced or suppressed by using localized pumping profiles. The operation of these devices relies on the whereabouts of the so-called exceptional points (EPs). These points are non-Hermitian degeneracies that occur when two or more eigenvalues and their corresponding eigenvectors coalesce [12]. Mathematically, they represent algebraic branch-cut singularities at which the eigenvector space ceases to be complete [12,13]. Recently, it was shown that lasing near EPs can lead to laser self-termination in coupled photonic molecules [14,15]. Interestingly, it was found that this effect can be fully understood by using linear coupled-mode formalism [16]. The work in Ref. [16] also provides a means for understanding and controlling the lasing properties of parity-time reversal (*PT*) symmetric photonic molecule lasers made of multiple photonic cavities. More recently, the concept of *PT* symmetry was also invoked to build single longitudinal mode microring laser systems [17,18].

In this context, it is interesting to note that the problem of laser oscillations in coupled photonic structures dates back to a few decades ago. In fact, waveguide laser arrays have been a subject of intense investigations for the purpose of building high-power phase-locked lasers [19–22]. However, it was shown that their operation is dominated by multimode chaotic emission [20]. In general, the longitudinal modes associated with each cavity can be eliminated by using distributed Bragg gratings (DBG) [23] or periodic *PT* symmetric structures [18]. On the other hand, eliminating the transverse collective modes of the array is a daunting job. While several methods have been proposed to overcome this obstacle and regulate the functionalities of these devices [24–26], controlling their emission characteristics by using practical schemes remains an open problem.

In this work we propose a scheme for filtering the undesired transverse supermodes of laser arrays by using the concept of SUSY and we analyze their optical properties at the lasing threshold. Our analysis is based on a steady-state semiclassical laser theory that can account for lasing frequency, threshold, output power, as well as other properties [16,27,28]. Fully quantum treatments [29] that are necessary for investigating features such as the laser linewidth will be carried out elsewhere. Finally, we also investigate the robustness of the proposed structure against lattice disorder and nonlinear effects.

II. SINGLE-MODE LASING IN SUPERSYMMETRIC LASER ARRAYS

Laser arrays are devices that consist of several interacting laser cavities [19–22]. In integrated optics platforms, these cavities are usually made of waveguides, ring resonators, or photonic crystal cavities. In typical laser arrays, all the cavities are pumped equally with an external power source which results in multimode oscillations. Later, selective current injection was proposed as a means to favor the emission of only one mode [24]. Here we propose a different and more

*ganainy@mtu.edu

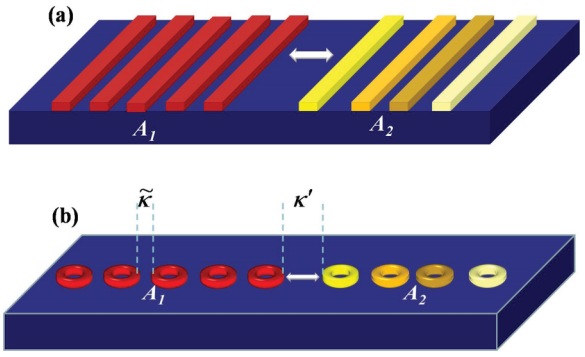

FIG. 1. (Color online) A schematic of possible physical realizations of supersymmetric laser arrays using (a) a waveguides platform and (b) optical resonator configurations.

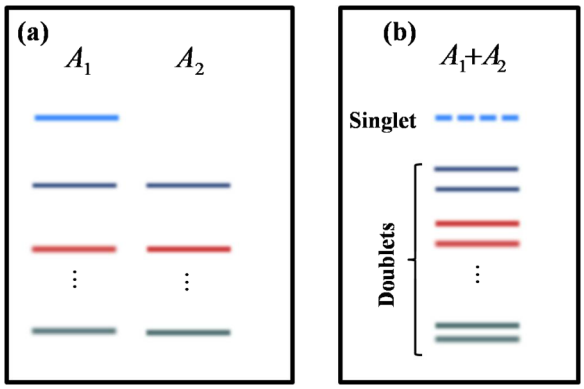

FIG. 2. (Color online) Conceptual demonstration of singlet lasing using a supersymmetric array. (a) A schematic of the individual spectra of an optical array and its superpartner that does not share the singlet state (with highest frequency). (b) The spectrum of the combined system. It consists of a set of doublets and one singlet. When optical loss is added to the superpartner lattice, supermode coupled-mode theory (SCMT) predicts that the singlet state (dashed line) will exhibit the lowest lasing threshold.

straightforward approach to achieve single transverse mode operation, i.e., by engineering the non-Hermiticity of the laser arrays to achieve mode selection through supersymmetry.

Figures 1(a) and 1(b) depict two different realizations of the proposed structure in both optical waveguide and cavity platforms. In contrast to previous studies in laser arrays, our proposed device consists of an optical lattice A_1 and a spectrally engineered auxiliary array A_2 that serves as a non-Hermitian loss element to suppress the unwanted transverse modes. In order to explain the principle of operation, we assume that the main array A_1 is made of N coupled identical cavities, each having the same linear mode. The coupling lifts the N-fold degeneracy and results in N linear supermodes of different frequencies. These modes can contribute to the lasing process [22], and this multimode character is the main reason for the chaotic emission in laser arrays [20]. In order to achieve stable steady-state lasing, all but one of these N linear modes must be eliminated (we will refer to them as E modes) to allow only one remaining mode (L mode) to participate in the lasing action. Thus, in order for the auxiliary array A_2 to achieve this required task, it should provide three functionalities: (1) it should increase the thresholds of the undesired E modes of A_1; (2) it should exhibit minimum influence on the desired L mode, and (3) it should not introduce other linear modes of lower threshold. While different optimization techniques might be invoked to achieve these goals, discrete supersymmetry (DSUSY) [4] provides a straightforward solution without the complications and constraints of numerical optimization.

More specifically, by applying the DSUSY prescription as described in Appendix A, we design the auxiliary array A_2 such that it has N-1 linear modes that have the same frequencies as the E modes of the main array A_1 [see Fig. 2(a)] but with stronger loss. By coupling these two arrays, for example, through their innermost cavities as shown in Fig. 1, the E modes of A_1 and their counterparts of A_2 form N-1 doublet states as shown in Fig. 2(b), and more importantly, these doublets have a stronger loss than the desired L mode; the latter does not couple to the auxiliary array and forms a singlet state. This singlet state lases when the pump power reaches its threshold, which is below those of the doublet states.

Before we analyze the system described in Fig. 1, we note that our proposed structure is conceptually different from those that rely on the typical Vernier effect [30]. In the latter, two cavities of different free spectral ranges are coupled, and frequency-mismatched resonances of these two cavities are eliminated by destructive interference. On the other hand, the suppressed modes in the design presented here are due to their increased thresholds, caused in turn by an additional loss introduced in a partner array, and interference does not play a role. The supersymmetry enables us to apply this additional loss to any chosen set of modes in the main array, without affecting the remaining one that becomes the singlet lasing mode. Hence it allows for unprecedented control over the single-mode operation regime.

III. LINEAR THRESHOLD ANALYSIS AND NUMERICAL SIMULATIONS

In order to investigate the lasing properties of the SUSY array structure proposed in the previous section, we employ the linear threshold analysis and we consider specific numerical examples. Conceptually, any laser system is composed of certain geometries that exhibit loss, gain, and feedback. In the absence of the gain, the complex eigenvalues of the system exist in the lower half of the complex plane, and any initial excitation will decay exponentially with time. As the gain is increased gradually, the eigenvalues are pulled toward the real axis. The linear threshold of each mode is defined as the gain value at which the eigenfrequency of this mode becomes real, which results in a steady-state laser oscillation. Once the linear thresholds of all possible lasing modes are considered, the value of the smallest one gives the actual lasing threshold, and its difference with the next smallest threshold is a good measure of how strong the gain can be increased before more than one lasing mode is excited. In other words, this difference gives an estimate of the range of gain value for single-mode operation. This treatment is a good approximation and has been widely used [22] because the laser is a linear system at the actual (first) threshold, at which the lasing intensity is zero. Nonlinear interactions will be treated in Sec. VI.

Achieving single-mode operation thus requires one to either pull only one mode preferably to the real axis as the gain increases while leaving other modes intact, or to push the undesired modes further down in the complex eigenvalue space by adding additional loss channels, which can be described as "selective Q-spoiling." While techniques based on selective mode pumping follow the first approach, our proposal here highlights the second strategy by introducing extra optical loss in the auxiliary array, for example, by depositing metallic films on top of its constitute cavities, which convert light intensity into heat. An alternative route for obtaining similar effects is to use deep Bragg gratings [31] that introduce optical losses by coupling light efficiently to the continuum radiation without producing excessive heat.

In order to confirm the validity of our approach, we consider a concrete example of an optical array made of five cavities having the same resonant frequency ω_o and a uniform intercavity coupling coefficient $\tilde{\kappa}$. The auxiliary SUSY partner of this structure can be constructed by using DSUSY as described in Appendix A, and the desired L mode is chosen to be the fundamental mode with the highest frequency. Next we assume that intracoupling between the main and auxiliary array is given by $\kappa'/\tilde{\kappa} = 0.2$ while the loss coefficient of the SUSY array is taken to be $\gamma_t = \gamma + \gamma_o$, where $\gamma = 0.06\,\tilde{\kappa}$, and γ_o represents the original loss of the individual cavities, as described in detail in the next section. Figure 3(a) depicts the normalized complex eigenvalue spectrum of this composite structure as obtained from the exact discrete system (blue triangles) when the applied uniform gain value across both arrays is equal to γ_o. As expected, only the singlet eigenmode reaches the lasing threshold (i.e., the real axis of the complex eigenvalue plane), and the doublet states are pushed down away from the real axis, indicating their higher thresholds. This behavior, denoted schematically by the dashed line in Fig. 2(b), is in direct contrast with the spectral distribution of eigenmodes of laser arrays in the absence of the auxiliary non-Hermitian SUSY partner array, where all the modes starts to lase at the same gain threshold. Evidently, our strategy succeeds in achieving single transverse mode lasing in a straightforward manner that does not require any special fabrication technology or complex nonuniform current injection schemes.

We further confirm these conclusions by investigating the temporal dynamics of proposed geometry under an initial arbitrary noise distribution as shown in Fig. 3(b). Clearly, as time evolves, all the higher-order optical eigenmodes suffer from dissipation and only the optical power obtained by projecting the initial noise distribution on the fundamental supermode survives. Note that only the main array A_1 is shown in Fig. 3(b) since the signal in the superpartner structure remains very weak during evolution.

As we have shown, both spectral analysis and temporal dynamics for the above example confirm single-mode operation of laser arrays when a SUSY partner structure is introduced as an additional loss channel for the undesired E modes without affecting the desired L mode. Therefore, our approach can have a significant impact on both the fundamental science aspect and industry applications of laser arrays. Below we present the analytical results of the SUSY arrays and compare them with the numerical simulations presented above.

IV. ANALYTICAL RESULTS: SUPERMODE COUPLED EQUATIONS FOR SUSY ARRAYS

In order to gain better understanding of the numerical linear threshold analysis presented above, we develop a supermode coupled-mode theory (SCMT) that treats the interaction between the supermodes of both arrays rather than dealing with the evanescent coupling between individual cavities. In this context, we note that the strength of the interaction between the supermodes is governed rather by their spatial overlap, which varies from one doublet to another.

We start our analysis by denoting the eigenvectors of the main array by $\vec{V}_m = [v_{m,1} \quad v_{m,2} \quad \ldots \quad v_{m,N-1} \quad v_{m,N}]^T$ and those of its superpartner lattice by $\vec{U}_l = [u_{l,1} \quad u_{l,2} \quad \ldots \quad u_{l,N-2} \quad u_{l,N-1}]^T$, where the integers

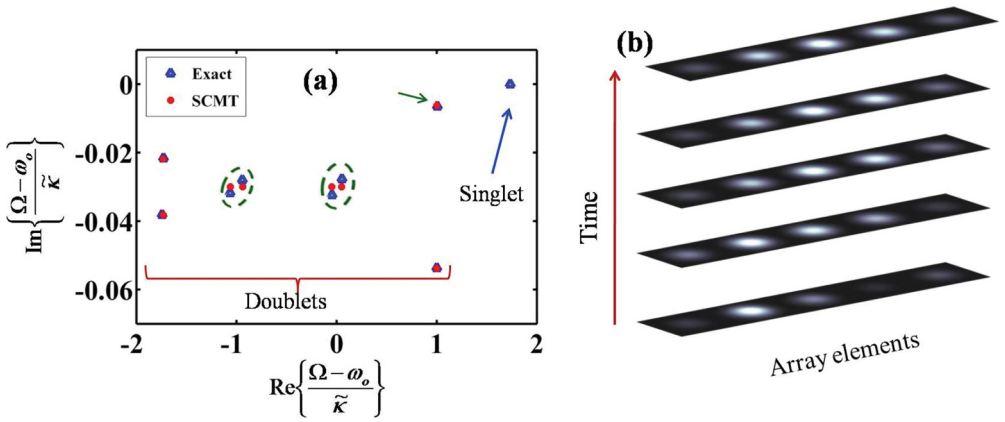

FIG. 3. (Color online) (a) Eigenvalue spectrum of a supersymmetric array when $\kappa'/\tilde{\kappa} = 0.2$ and $\gamma/\tilde{\kappa} = 0.06$, where $\tilde{\kappa}$ is the uniform coupling coefficients between the cavities of the original array, κ' is the coupling constant between the innermost channels of the main lattice and its superpartner, while γ is the uniform optical loss coefficient of the superpartner structure A_2. Results obtained using exact diagonalization of the discrete system and from supermode coupled-mode theory (SCMT) are compared on the same figure. (b) Temporal evolution of an initial arbitrary optical intensity distribution in this SUSY array. As expected, only the fundamental eigenmode of A_1 survives as time lapses. Only the optical cavities of the array A_1 are depicted.

m and l take the values $1 \leqslant m \leqslant N$ and $1 \leqslant l \leqslant N-1$, respectively. Here, N is the total number of optical cavities of the main lattice and the superscript T denotes matrix transpose. If the spectrum of the SUSY array is constructed as described in Appendix A where the fundamental optical mode does not have a superpartner mode, the optical tunneling can be assumed to occur only between $\vec{V}_{l+1}$ and $\vec{U}_l$. By denoting the coupling coefficients between the innermost cavities as given by κ', we find that the overlap between the supermodes $\vec{V}_{l+1}$ and $\vec{U}_l$ is given by $\kappa_l = v_{l+1,N}\,\kappa'\,u_{l,1}$, where the magnitudes of the eigenvectors have been normalized to unity. The SCMT between the degenerate eigenstates of both arrays (the ones that form a doublet) now takes the following form:

$$\begin{aligned} i\frac{dV_{l+1}}{dt} - \omega_l V_{l+1} - \kappa_l U_l = 0, \\ i\frac{dU_l}{dt} - \omega_l U_l + i\gamma\, U_l - \kappa_l V_{l+1} = 0. \end{aligned} \tag{1}$$

Here V_{l+1} and U_l are scalar quantities that represent the modal amplitude associated with the two eigenvectors $\vec{V}_{l+1}$ and $\vec{U}_l$, respectively, while ω_l is their resonant frequency. We note that each of the $(2N-1)$ cavities in the array can support more than one ω_l in general, but here we focus on the single-mode case where only one of them is relevant, which can be achieved using DBG [23] or periodic PT symmetric structures [18]. In Eq. (1), we have also introduced the γ term to account for a uniform and stronger optical loss in the superpartner lattice as described in Sec. II. The original homogenous loss of the individual cavities can be neglected at first in our analysis, since it can be included simply as an imaginary part of ω_l, which causes the same threshold increase of all modes. We come back to this issue later when discussing the quantitative difference between the thresholds of the singlet state and the doublet states.

The eigenvalues associated with Eq. (1) that vary as $\exp(-i\,\Omega\,t)$ are given by $\Omega_l^{\pm} = [\omega_l \pm \sqrt{\kappa_l^2 - (\frac{\gamma}{2})^2}] - \frac{\gamma}{2}i$. Clearly two distinct regimes can be identified for the eigenvalues depending on the ratio between κ_l and γ. When $\kappa_l/\gamma > 0.5$, any two resonances belonging to the same doublet will have the same resonant lifetime $2/\gamma$ and their frequency split is given by $\Delta\Omega_l = \Omega_l^+ - \Omega_l^- = 2\sqrt{\kappa_l^2 - (\frac{\gamma}{2})^2}$. In this regime, doublet states are formed as symmetric and antisymmetric superposition of the supermodes of the two individual lattices, and hence both have similar intensity distributions. On the other hand, when $\kappa_l/\gamma < 0.5$, the two eigenmodes share the same resonant frequency while their resonance bandwidth ($\mathrm{Im}\{\Omega_l^{\pm}\}$) becomes different and their intensity distribution becomes strongly localized in either the main array or its superpartner structure. This phase transition is known as spontaneous PT symmetry breaking [32–42]. The onset of this transition at the point $\kappa_l/\gamma = 0.5$ is marked by an exceptional point [12,13]. Note that according to the above model, the singlet eigenmode will always have zero loss. On the other hand, the loss factor of any of the doublets remains finite and approaches zero only in the limit when $\kappa_l/\gamma \ll 1$. This immediately suggests that the singlet supermode exhibits lower lasing threshold than any other eigenmode in the spectrum. Figure 3(a) depicts the eigenvalue spectrum of the array considered in Sec. II by using SCMT, as shown by the red dots. Evidently good agreement between the exact diagonalization and the SCMT is observed in most cases. Note also that SCMT predicts the nonuniform splitting of the doublets. However, some small discrepancies between both calculations do exist, as indicated by the closed dashed curves. We show in Appendix B that this is an outcome of nonresonant interactions using the Brillouin-Wigner (BW) perturbation method [43].

These results thus quantify and confirm the possibility of achieving lasing action only in the singlet state by applying a uniform optical gain to all the cavities. To calculate the lowest threshold of the doublet states in comparison with the singlet, we denote the initial material and radiation loss in every individual cavity in both lattices by γ_0. By adding the extra loss γ to the superpartner structure as described in Sec. II, its total loss becomes $\gamma + \gamma_0$. Evidently, γ_0 increases the thresholds of all modes in the SUSY array by the same amount. The singlet state reaches threshold when the applied gain, denoted by g_s, equals γ_0. The lower threshold for a pair of doublet states $\Omega_l^{\pm}$, denoted by g_l and calculated using SCMT in the absence of nonlinear interactions, is given by $g_l = \gamma_0 + \frac{\gamma}{2} - \sqrt{(\frac{\gamma}{2})^2 - \kappa_l^2}$ in the PT broken phase and $g_l = \gamma_0 + \frac{\gamma}{2}$ in the PT symmetric phase. For a given structure (and hence κ_l), clearly $g_l(\gamma)$ reaches its maximum value right at the EP when $\gamma = 2\kappa_l \equiv \gamma^{EP}$. Under these favorable conditions for suppressing the doublet modes from lasing, the maximum ratio of the lowest doublet threshold and the singlet threshold is given by $1 + \frac{\kappa_l}{\gamma_0}$. From this analysis, it is clear that a strong coupling κ_l and a low loss γ_0 in the main array facilitates a significant single-mode lasing action. As we noted before, using this linear analysis to predict the lasing threshold is a well-established technique and has been verified before in literature [16,22]. However, in order to simulate emission dynamics beyond the lowest lasing threshold, one has to resort to more complicated nonlinear models. Nevertheless, it is reasonable to expect that in a SUSY array the saturated gain medium in the main lattice will further suppress the doublet states from lasing [27].

Finally, we note that the loss parameters γ_0 and γ depend on the individual mode of each cavity that make up the composite supermodes of the whole array. These parameters can vary significantly for different individual cavity modes in the same cavity, including in a wave-chaotic cavity [44]. We have also neglected the effects arising from the so-classed external coupling between cavities, which can change the effective loss of the supermodes in the main array before the SUSY array is introduced [45].

V. ROBUSTNESS AGAINST ARRAY DISORDER

It is very well known that disorder effects can have a profound influence on the structure of the eigenmodes and the energy exchange dynamics in continuous and discrete systems [46]. Processes such Anderson localization [47] and transition between ballistic and diffusive propagation have been observed in discrete waveguide arrays [48]. In this section we investigate the robustness of our proposed supersymmetric laser array against these disorder effects. In order to do so, we have introduced a random disorder on the coupling parameters and resonant frequencies of all the array elements in steps ranging from $\pm 1\%$ up to $\pm 20\%$ in units of $\tilde{\kappa}$. These random values

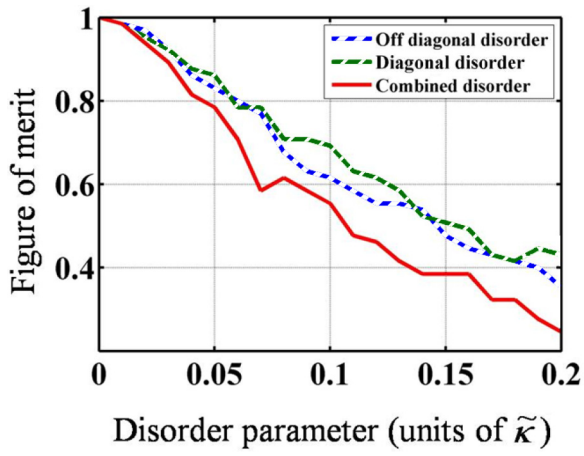

FIG. 4. (Color online) The effect of the disorder on the maximum possible gain value before the second mode starts to lase, when the disorder is introduced to the coupling coefficients only or the resonant frequency only, are indicated by the blue dotted (middle) line and the green dashed line, respectively. The combined effects are shown by the red solid curve. The figure of merit is defined as the relative spacing between the gain threshold of the first and second lasing modes in the disordered case compared to the ideal case, i.e., $\frac{(g_1^{th}-g_2^{th})_{\text{disorder}}}{(g_1^{th}-g_2^{th})_{\text{ideal}}}$. The system still displays a good range of single-mode operation at disorder levels of up to 10% of the value of $\tilde{\kappa}$. The current fabrication technique allows for building waveguide or cavity arrays with such accuracy.

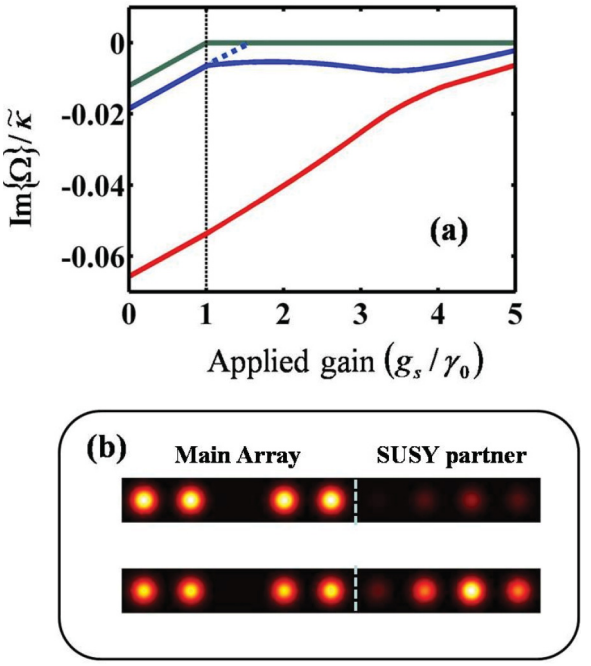

FIG. 5. (Color online) (a) Increased range of single-mode operation due to nonlinear spatial hole burning interactions. The system is the same as in Fig. 3, and we have considered a uniform loss $\gamma_0 = \gamma/5$ in all cavities. The top solid line shows the singlet state, and the other two solid lines show the doublet pair next to it in frequency. The dotted line indicates the effective gain of the lower-loss one of them in the absence of nonlinear interactions. The vertical dashed line marks the threshold of the singlet state. (b) Spatial profile of the lower-loss doublet state when $g_s = 0$(top) and γ (bottom).

were picked from a uniform distribution, and an averaging of a hundred different realizations was computed for each step. In Fig. 4, the blue dotted (middle) line depicts the results when the disorder is introduced only in the coupling coefficients (off-diagonal elements of the discrete Hamiltonian), which correspond to fabrication errors in the distance between the waveguides. The green dashed curve in the same figure represents the case when the disorder is introduced in the diagonal element of the Hamiltonian, corresponding to the resonant frequencies which result from fabrication errors in the waveguide length. Finally, the combined effect of both transverse and longitudinal disorders is shown by the red solid line. The figure of merit in Fig. 4 is defined as the difference between the lasing threshold of the first and second lasing modes in the disordered case relative to the ideal case, i.e., $\frac{(g_1^{th}-g_2^{th})_{\text{disorder}}}{(g_1^{th}-g_2^{th})_{\text{ideal}}}$. We note that the device performance defined by the figure of merit drops linearly as a function of the disorder parameter. However, as indicated by our simulations, a considerable single-mode operation domain can be still achieved even when the disorder parameter is $\tilde{\kappa}/10$. Given the precise fabrication techniques available these days [49], it is not a difficult task to fabricate these structures with the necessary accuracy for optimal operation.

VI. NONLINEAR EFFECTS

In Sec. III we discuss the linear threshold analysis of the proposed supersymmetric laser array. As we mentioned earlier, strong nonlinear interactions between the first lasing mode and the competing ones can increase the range of single-mode lasing in terms of the applied gain g_s. In order to confirm this statement, here we consider spatial hole burning interactions and show that it can indeed increase this range considerably. Intuitively, this can be understood by recalling that the applied gain is partially depleted by the lasing mode: the stronger the laser intensity in a given cavity, the more depleted the applied gain becomes in that cavity. This saturation can be modeled by $\frac{g_s}{1+|\Psi_i^2|}$, where Ψ_i is the (complex-valued) field amplitude of the lasing mode in the ith cavity. As an example, we consider the case of $\gamma = 5\gamma_0$, where we find the nonlinear effects to be strong. We calculate Ψ_i as a function of the applied gain g_s by using the techniques developed in the steady-state *ab-initio* laser theory (SALT) [27,28]. In these calculations, we assumed uniform pumping across both arrays. Our analysis shows that the lasing threshold of the singlet state is reached when $g_s = \gamma_0$, the uniform loss assumed for both the main array and its SUSY partner array. When the applied gain is increased beyond this threshold value ($g_s > \gamma_0$), the corresponding eigenvalue of the lasing mode stays real [see the topmost green line in Fig. 5(a)]. On the other hand, the next competing mode will not start to lase until its eigenvalue also reaches the real axis. According to the results of the linear analysis shown in Fig. 3, the next lasing mode corresponds to one of the doublet states (indicated by the green arrow). If the nonlinear effects were absent, this state would start lasing at $g_s \approx 1.53\gamma_0$, as indicated by the dotted blue line in Fig. 5(a). However, when the spatial hole burning interactions are taken into account, the saturated gain increases the threshold of this doublet state

considerably, as can be seen from the solid blue curve in Fig. 5(a). Moreover, soon after the first mode starts lasing, the gain saturation becomes so strong that the effective gain felt by this mode even decreases with g_s, before it eventually increases again as g_s is further increased. During the latter process, the mode intensity becomes enhanced in the SUSY partner array that exhibits stronger loss [see Fig. 5(b)]. This behavior delays the onset of this doublet state, and it does not lase even when the applied gain is five times the threshold of the first lasing mode. For completeness we also show the behavior of the second mode of this doublet state [red line in Fig. 5(a)]. A similar trend is also observed for the other doublet states (not shown), which verifies the robustness of singlet-mode lasing against nonlinear effects in our proposed structure.

Finally, we would like to comment on the feasibility of the proposed structure for high-power applications. In general, nonlinear Kerr interactions inside single cavities can lead to effects such as filamentation [50]. The advantage of using laser arrays is that the total optical power is distributed between several resonators and hence the Kerr nonlinear interactions are reduced compared to that of a single element laser having the same output power. We also note that all the technologies that are used to suppress filamentation in single-cavity lasers can be applied to laser arrays.

VII. DISCUSSION AND CONCLUSION

The SCMT presented above provides a consistent picture with our physical intuition. For certain design parameters, however, exceptions take place where the lasing mode having the lowest threshold turns out to be a doublet state. This finding is exemplified in Fig. 6, where the singlet state has the second highest frequency. As we show in Appendix B using the Brillouin-Wigner perturbation method [43], these rare exceptions are due to nonresonant interactions between multiple supermodes in the main array and the auxiliary array, a feature that was previously overlooked in the study of supersymmetric optical structures. We note, however, that in the scenario presented in Fig. 6, the singlet state is one of the higher-order modes while the first lasing state is still the fundamental mode. If the fundamental mode is chosen to be the singlet state, our simulations show that the rare exceptions mentioned above do not arise. Given that lasing emission from the fundamental optical mode is usually preferable in realistic systems, these rare exceptions do not pose any challenge.

In presenting the scheme and analysis of SUSY arrays above, we have assumed a uniformly applied gain in both the main and auxiliary arrays while introducing a stronger loss in the latter. Another alternative to favor lasing in the singlet state is to uniformly pump only the main array, without the need to introduce additional loss to the auxiliary array. In this case, the threshold of the singlet state remains the same at $g_s = \gamma_0$, since it does not couple to the superpartner lattice. On the other hand, the eigenfrequencies of the doublet states as obtained by using the SCMT are now given by $\Omega_l^{\pm} = [\omega_l - i\gamma_0 \pm \sqrt{\kappa_l^2 - (\frac{g}{2})^2}] + \frac{g}{2}i$. Clearly, when $\gamma_0 < \kappa_l$ the doublet reaches their lasing threshold at $g_l = 2\gamma_0$ and remains in the PT symmetric phase. Otherwise (i.e., when $\gamma_0 > \kappa_l$), the pair starts to lase in the PT broken phase and

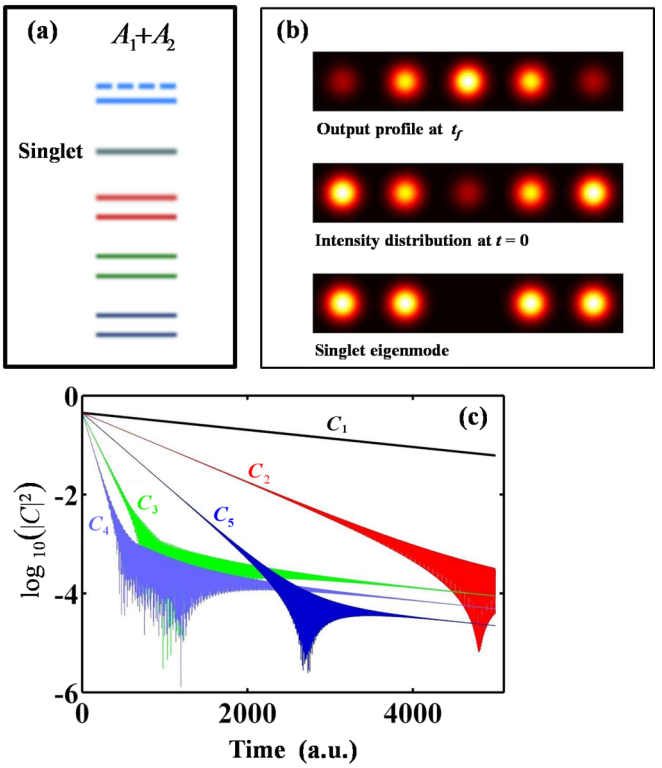

FIG. 6. (Color online) (a) Eigenvalue distribution of a supersymmetric array made of nine resonators (five of which belong to A_1) designed to eliminate the second-order eigenmode of A_1 from the spectrum of A_2. In this example, $\kappa'/\tilde{\kappa} = 0.2$ and $\gamma/\tilde{\kappa} = 0.5$. The doublet state indicated by the dashed line reaches the lasing point before the singlet state, in contrary to what one would expect. This counterintuitive result is confirmed in (b), where an initial state made of an equal superposition of the five eigenmodes of A_1 (middle panel) evolves to the doublet eigenstates (upper panel) instead of the singlet (lower panel). Panel (c) presents the time-dependent dynamics for the projection coefficients $C_n(t)$, defined by $\vec{\varphi}(t) = \sum_{n=1}^{N} C_n(t)\ \vec{V}_n$ in the main array. $C_n(t = 0) = 1/\sqrt{5}$ for all n.

their lower threshold is given by $g_l = \gamma_0 + \frac{\kappa_l^2}{\gamma_0} < 2\gamma_0$ [16]. Thus, for a given loss coefficient γ_0 in every individual cavity of both arrays, operation in the PT symmetric phase is more favorable to suppress lasing in the doublet states, achievable by making κ_l greater than γ_0. Within this scenario, the maximum ratio of the lower doublet threshold and the singlet threshold in the linear analysis is then exactly 2.

In conclusion, we have introduced the concept of SUSY laser arrays that are capable of supporting laser oscillations in the singlet states only. If each cavity of the SUSY array supports only a single resonant frequency [18,23], then single-mode lasing is possible in the corresponding singlet state. We have also shown that under certain operation conditions, anomalous lasing can occur where one of the doublet eigenmodes exhibits a lower lasing threshold than the singlet state due to nonresonant interactions.

ACKNOWLEDGMENT

L.G. acknowledges support by PSC-CUNY 46 Research Grant from the City University of New York.

APPENDIX A: CONSTRUCTION OF A SUPERSYMMETRIC PARTNER ARRAY

In order to construct the supersymmetric auxiliary lattice, we note that the Hamiltonian of the main array A_1 can be described by a discrete $N \times N$ tridiagonal Hamiltonian matrix $H^{(1)}$ whose elements are given by $H^{(1)}_{n,n} = \omega_o$ and $H^{(1)}_{n,n+1} = H^{(1)}_{n+1,n} = \tilde{\kappa}$. The Hamiltonian of its superpartner structure that does not contain the mth mode of A_1 can be constructed through discrete SUSY transformation [4,5], and it is given by $H^{(2)} = (RQ + \omega_m I)_{(N-1)} = (Q^T H^{(1)} Q)_{(N-1)}$, where ω_m is the eigenfrequency of the mth mode of A_1 and I is the unit matrix of dimensions $N \times N$. The subscript indicates that $H^{(2)}$ is constructed by selecting only the upper-left block diagonal matrix of dimensions $(N-1) \times (N-1)$ of the larger matrix in the parentheses after isolating the zero mth eigenvalue at the last row and column. Here Q and R are the QR factorization matrices of $H^{(1)} - \omega_m I$ [51].

APPENDIX B: BRILLOUIN-WIGNER PERTURBATION ANALYSIS FOR SUSY ARRAYS AND NONRESONANT INTERACTIONS

In order to understand the difference of the numerical simulation and SCMT in Fig. 3(a), and more importantly, the change of lasing order briefly mentioned in the conclusion section of the main text, we analyze the SUSY array using a perturbation theory. We start by writing the total Hamiltonian of the system in the following form:

$$H_{\rm tot} = H_o + H_I,$$
$$H_o = \begin{bmatrix} H_1 & 0 \\ 0 & H_2 \end{bmatrix} \quad \text{and} \quad H_I = \begin{bmatrix} 0 & Z \\ Z^T & 0 \end{bmatrix}. \tag{B1}$$

In Eq. (B1), H_o is the unperturbed Hamiltonian and is part of a closed algebra [2], while H_I is a Hermitian perturbation that couples the main array A_1 to its superpartner lattice A_2. Z is in general an $N \times (N-1)$ matrix ($N = 5$ in the examples given in the main text), with $z_{N,1} = \kappa'$ and zero entries otherwise. In principle, one can apply the usual Rayleigh-Schrodinger (RS) perturbation theory [52] to study the eigenvalues and eigenmodes of $H_{\rm tot}$. However, the procedure is complicated by the multiple twofold degeneracies associated with H_o. A powerful alternative is to employ Brillouin-Wigner (BW) perturbation method [43]. While both RS and BW perturbation methods agree to first order, the BW method offers more accurate results for higher-order calculations with the need for any special treatments for degenerate eigenstates. These advantages come at the expense of solving polynomial equations in order to obtain the perturbed eigenvalues. In particular, the expression for the new eigenvalues using the BW method takes the form

$$\begin{aligned}
\Omega_l^{\rm new} &= \Omega_l + \sum_{j=1}^{\infty} S_j, \\
S_1 &= \vec{W}_l^T H_I \vec{W}_l, \\
S_2 &= \sum_{m \neq l} \frac{\left(\vec{W}_l^T H_I \vec{W}_m\right)\left(\vec{W}_m^T H_I \vec{W}_l\right)}{\Omega_l^{\rm new} - \Omega_m}, \\
&\vdots \\
S_{j+1} &= \sum_{m_1 \neq l} \sum_{m_2 \neq l} \sum_{m_j \neq l} \frac{\left(\vec{W}_l^T H_I \vec{W}_{m_1}\right)\left(\vec{W}_{m_1}^T H_I \vec{W}_{m_2}\right) \ldots \left(\vec{W}_{m_j}^T H_I \vec{W}_l\right)}{\left(\Omega_l^{\rm new} - \Omega_{m_1}\right)\left(\Omega_l^{\rm new} - \Omega_{m_2}\right) \ldots \left(\Omega_l^{\rm new} - \Omega_{m_j}\right)},
\end{aligned} \tag{B2}$$

where Ω_m and $\vec{W}_m$ are the unperturbed eigenvalues and eigenvectors of H_o, respectively, and $\Omega_l^{\rm new}$ is the new perturbed eigenfrequency associated with the lth mode. The subscripts m_i in the summation for the S_j terms run over all the modes of the systems except the indicated ones. As we have noted, the spectrum of H_o contains multiple double degeneracies. Thus the eigenvector bases are not unique. Here we use the bases $\left[\begin{smallmatrix} \vec{V}_{l_1} \\ \vec{0}_{4\times 1} \end{smallmatrix}\right]$ and $\left[\begin{smallmatrix} \vec{0}_{5\times 1} \\ \vec{U}_{l_2} \end{smallmatrix}\right]$, where the subscripts $l_{1,2}$ run over all the modes of $H_{1,2}$, respectively, and $\vec{V}_{l_1}$ and $\vec{U}_{l_2}$ are their associated eigenvectors. Here $\vec{0}_{n\times 1}$ is a column vector of dimensions $n \times 1$. In these bases, the first-order correction T_1 in the above formula is zero for our problem. Interestingly, if we restrict our perturbation expansion to a second-order approximation and we retain only the resonant term in the summation of T_2 (i.e., the term that satisfies $\mathrm{Re}\{\Omega_l - \Omega_m\} = 0$), Eq. (B2) reduces to the SCMT and the two eigenfrequencies $\Omega_l^{\pm}$ described above emerge naturally as solutions of a quadratic equation. However, in order to proceed beyond the SCMT, one has to consider the full polynomial equation with all its possible solutions. These solutions can be found graphically or by using any of the well-developed numerical techniques. Among this family of solutions, only those that represent relatively small perturbation over the unperturbed eigenmode should be retained while the others must be discarded.

A simpler procedure for finding the relevant solutions can be obtained by noting that in our particular SUSY configuration, the strongest contributions to the expansion (B2) arise from the interaction between resonant modes. By neglecting terms higher than T_2 and substituting $\Omega_l^{\rm new} = \Omega_l$ in every term in the right-hand side of T_2 except the resonant one, we arrive at a quadratic equation whose two solutions are

given by

$$\Omega_l^{\text{new}} = \frac{\Omega_l + \Omega_n + \delta}{2} \pm \sqrt{\left|\left(\vec{W}_n^T H_I \vec{W}_l\right)\right|^2 + \left(\frac{\Omega_l + \delta - \Omega_n}{2}\right)^2}, \quad \text{(B3)}$$

where the complex parameter $\delta = \sum_{m \neq l,n} \frac{|(\vec{W}_m^T H_I \vec{W}_l)|^2}{\Omega_l - \Omega_m}$ characterizes the second-order interaction between nonresonant SUSY eigenstates while the resonant eigenvalue Ω_n satisfies the relation $\text{Re}\{\Omega_l - \Omega_n\} = 0$. We verify formula (B3) by first revisiting the example of Fig. 3. Recall that in contradiction with the exact diagonalization of the full discrete Hamiltonian, SCMT did not account for PT spontaneous symmetry breaking of some of the doublets in the spectrum, as highlighted by the dashed closed curves in Fig. 3(a). Equation (B3), on the other hand, correctly predicts the onset of PT phase transition in both cases. Finally, by applying the BW perturbation analysis of Eq. (B3) to the example associated with Fig. 6, we find that BW analysis remarkably reproduces the unexpectedly anomalous spectrum with high accuracy. It is thus clear that the counterintuitive shuffling of the orders of the lasing modes indicated schematically in Fig. 6(a) is a direct outcome of the nonresonant interactions between the modes [42].

[1] S. Weinberg, *The Quantum Theory of Fields, Supersymmetry* (Cambridge University Press, Cambridge, UK, 2005), Vol. 3.

[2] F. Cooper, *Supersymmetry in Quantum Mechanics* (World Scientific, Singapore, 2002).

[3] J. Radovanović, V. Milanović, Z. Ikonić, and D. Indjin, Quantum-well shape optimization for intersubband-related electro-optic modulation properties, Phys. Rev. B **59**, 5637 (1999); J. Bai and D. Citrin, Supersymmetric optimization of second-harmonic generation in mid-infrared quantum cascade lasers, Opt. Exp. **14**, 4043 (2006).

[4] M. A. Miri, M. Heinrich, R. El-Ganainy, and D. N. Christodoulides, Supersymmetric Optical Structures, Phys. Rev. Lett. **110**, 233902 (2013).

[5] M. Heinrich, M. A. Miri, S. Stützer, R. El-Ganainy, S. Nolte, A. Szameit, and D. N. Christodoulides, Supersymmetric mode converters, Nat. Commun. **5**, 3698 (2014).

[6] X. Wu, J. Andreasen, H. Cao, and A. Yamilov, Effect of local pumping on random laser modes in one dimension, J. Opt. Soc. Am. B **24**, A26 (2007).

[7] J. Andreasen, C. Vanneste, L. Ge, and H. Cao, Effects of spatially nonuniform gain on lasing modes in weakly scattering random systems, Phys. Rev. A **81**, 043818 (2010).

[8] L. Ge, Y. D. Chong, S. Rotter, H. E. Türeci, and A. D. Stone, Unconventional modes in lasers with spatially varying gain and loss, Phys. Rev. A **84**, 023820 (2011).

[9] T. Hisch, M. Liertzer, D. Pogany, F. Mintert, and S. Rotter, Pump-Controlled Directional Light Emission from Random Lasers, Phys. Rev. Lett. **111**, 023902 (2013).

[10] L. Ge, Mode selection and single-mode lasing by active transformation optics, arXiv:1408.4827.

[11] S. F. Liew, B. Redding, L. Ge, G. S. Solomon, and H. Cao, Active control of emission directionality of semiconductor microdisk lasers, Appl. Phys. Lett. **104**, 231108 (2014).

[12] W. D. Heiss, Exceptional points of non-Hermitian operators, J. Phys. A **37**, 2455 (2004).

[13] M. Müller and I. Rotter, Exceptional points in open quantum systems, J. Phys. A **41**, 244018 (2008).

[14] M. Liertzer, L. Ge, A. Cerjan, A. D. Stone, H. E. Tureci, and S. Rotter, Pump-Induced Exceptional Points in Lasers, Phys. Rev. Lett. **108**, 173901 (2012).

[15] M. Brandstetter, M. Liertzer, C. Deutsch, P. Klang, J. Schöberl, H. E. Türeci, G. Strasser, K. Unterrainer, and S. Rotter, Reversing the pump dependence of a laser at an exceptional point, Nat. Commun. **5**, 4034 (2014).

[16] R. El-Ganainy, M. Khajavikhan, and Li Ge, Exceptional points and lasing self-termination in photonic molecules, Phys. Rev. A **90**, 013802 (2014).

[17] H. Hodaei, M. A. Miri, M. Heinrich, D. N. Christodoulides, and M. Khajavikhan, Parity-time–symmetric microring lasers, Science **346**, 975 (2014).

[18] L. Feng, Z. J. Wong, R.-M. Ma, Y. Wang, and X. Zhang, Single-mode laser by parity-time symmetry breaking, Science **346**, 972 (2014).

[19] J. K. Butler, D. E. Ackley, and D. Botez, Coupled-mode analysis of phase-locked injection laser arrays, Appl. Phys. Lett. **44**, 293 (1984).

[20] S. S. Wang and H. G. Winful, Dynamics of phase-locked semiconductor laser arrays, Appl. Phys. Lett. **52**, 1774 (1988).

[21] H. G. Winful and S. S. Wang, Stability of phase locking in coupled semiconductor laser arrays, Appl. Phys. Lett. **53**, 1894 (1988).

[22] E. Kapon, J. Katz, and A. Yariv, Supermode analysis of phase-locked arrays of semiconductor lasers, Opt. Lett. **9**, 125 (1984).

[23] J. E. Carroll, J. E. A. Whiteaway, and R. G. S. Plumb, *Distributed Feedback Semiconductor Lasers* (The Institution of Engineering and Technology, Stevenage Herts, UK, 1998).

[24] E. Kapon, J. Katz, S. Margalit, and A. Yariv, Controlled fundamental supermode operation of phase-locked arrays of gain-guided diode lasers, Appl. Phys. Lett. **45**, 600 (1984).

[25] M. Taneya, M. Matsumoto, S. Matsui, S. Yano, and T. Hijikata, 0° phase mode operation in phased-array laser diode with symmetrically branching waveguide, Appl. Phys. Lett. **47**, 341 (1985).

[26] L. Goldberg and J. F. Weller, Injection locking and single-mode fiber coupling of a 40-element laser diode array, Appl. Phys. Lett. **50**, 1713 (1987).

[27] H. E. Tureci, L. Ge, S. Rotter, and A. D. Stone, Strong interactions in multimode random lasers, Science **320**, 643 (2008).

[28] L. Ge, Y. D. Chong, and A. D. Stone, Steady-state *ab-initio* laser theory: Generalizations and analytic results, Phys. Rev. A **82**, 063824 (2010).

[29] M. O. Scully, *Quantum Optics* (Cambridge University Press, Cambridge, UK, 1997).

[30] K. J. Ebeling, L. A. Coldren, B. I. Miller, and J. A. Rentschler, Generation of single-longitudinal-mode subnanosecond light pulses by high-speed current modulation of monolithic two-section semiconductor lasers, Electron. Lett. **18**, 901 (1982); L. Ge and H. E. Tureci, Inverse vernier effect in coupled lasers, Phys. Rev. A **92**, 013840 (2015).

[31] B. E. Little, A variational coupled-mode theory including radiation loss for grating-assisted couplers, IEEE J. Lightwave Technol. **14**, 188 (1996).

[32] C. M. Bender and S. Boettcher, Real Spectra in Non-Hermitian Hamiltonians Having $\mathcal{PT}$ Symmetry, Phys. Rev. Lett. **80**, 5243 (1998).

[33] A. Znojil, $\mathcal{PT}$-symmetric square well, Phys. Lett. A **285**, 7 (2001).

[34] Z. Ahmed, Real and complex discrete eigenvalues in an exactly solvable one-dimensional complex $\mathcal{PT}$-invariant potential, Phys. Lett. A **282**, 343 (2001).

[35] R. El-Ganainy, K. G. Makris, D. N. Christodoulides, and Z. H. Musslimani, Theory of coupled optical $\mathcal{PT}$-symmetric structures, Opt. Lett. **32**, 2632 (2007).

[36] K. G. Makris, R. El-Ganainy, D. N. Christodoulides, and Z. H. Musslimani, Beam Dynamics in $\mathcal{PT}$ Symmetric Optical Lattices, Phys. Rev. Lett. **100**, 103904 (2008).

[37] Z. H. Musslimani, K. G. Makris, R. El-Ganainy, and D. N. Christodoulides, Optical Solitons in $\mathcal{PT}$ Periodic Potentials, Phys. Rev. Lett. **100**, 030402 (2008).

[38] K. G. Makris, R. El-Ganainy, D. N. Christodoulides, and Z. H. Musslimani, $\mathcal{PT}$-symmetric optical lattices, Phys. Rev. A **81**, 063807 (2010).

[39] A. Guo, G. J. Salamo, D. Duchesne, R. Morandotti, M. Volatier-Ravat, V. Aimez, G. A. Siviloglou, and D. N. Christodoulides, Observation of $\mathcal{PT}$ Symmetry Breaking in Complex Optical Potentials, Phys. Rev. Lett. **103**, 093902 (2009).

[40] C. E. Ruter, K. G. Makris, R. El-Ganainy, D. N. Christodoulides, M. Segev, and D. Kip, Observation of parity-time symmetry in optics, Nat. Phys. **6**, 192 (2010).

[41] Y. D. Chong, L. Ge, and A. D. Stone, $\mathcal{PT}$-Symmetry Breaking and Laser-Absorber Modes in Optical Scattering Systems, Phys. Rev. Lett. **106**, 093902 (2011).

[42] L. Ge and A. D. Stone, Parity-Time Symmetry Breaking Beyond one Dimension: The Role of Degeneracy, Phys. Rev. X **4**, 031011 (2014).

[43] S. Wilson and I. Hubac, *Brillouin-Wigner Methods for Many-Body Systems* (Springer, Berlin, 2012).

[44] G. Hackenbroich, C. Viviescas, and F. Haake, Field Quantization for Chaotic Resonators with Overlapping Modes, Phys. Rev. Lett. **89**, 083902 (2002).

[45] Q. H. Song and H. Cao, Improving Optical Confinement in Nanostructures via External Mode Coupling, Phys. Rev. Lett. **105**, 053902 (2010).

[46] A. Lagendijk, B. van Tiggelen, and D. S. Wiersma, Fifty years of Anderson localization, Phys. Today **62**, 24 (2009).

[47] M. Segev, Y. Silberberg, and D. N. Christodoulides, Anderson localization of light, Nat. Photon. **7**, 197 (2013).

[48] T. Eichelkraut, R. Heilmann, S. Weimann, S. Stützer, F. Dreisow, D. N. Christodoulides, S. Nolte, and A. Szameit, Mobility transition from ballistic to diffusive transport in non-Hermitian lattices, Nat. Commun. **4**, 2533 (2013).

[49] M. L. Cooper, G. Gupta, M. A. Schneider, W. M. J. Green, S. Assefa, F. Xia, Y. A. Vlasov, and S. Mookherjea, Statistics of light transport in 235-ring silicon coupled-resonator optical waveguides, Opt. Exp. **18**, 26505 (2010).

[50] J. R. Marciante and G. P. Agrawal, Nonlinear mechanisms of filamentation in broad-area semiconductor lasers, IEEE J. Quantum Electron. **32**, 590 (1996).

[51] J. E. Gentle, *Matrix Algebra: Theory, Computations, and Applications in Statistics* (Springer, Berlin, 2007).

[52] R. Shankar, *Principles of Quantum Mechanics* (Plenum Press, New York, 2011).